Title:

Unraveling the effects of spatial variability and relic DNA on the temporal dynamics of soil microbial communities

Authors:

Paul Carini[1,2], Manuel Delgado-Baquerizo[1,3], Eve-Lyn S. Hinckley[4,5], Tess E Brewer[1,6], Garrett Rue[4], Caihong Vanderburgh[1], Diane McKnight[4] and Noah Fierer[1,7]

Affiliations:

[1] Cooperative Institute for Research in Environmental Sciences, University of Colorado, Boulder, CO 80309

[2] Current Address: Department of Soil, Water and Environmental Science, University of Arizona, Tucson, AZ 85721

[3] Departamento de Biología y Geología, Física y Química Inorgánica, Escuela Superior de Ciencias Experimentales. Universidad Rey Juan Carlos, c/ Tulipán s/n, 28933 Móstoles, Spain.

[4]Institute of Arctic and Alpine Research, 4001 Discovery Dr, Boulder, CO 80303

[5]Environmental Studies Program, 4001 Discovery Dr, Boulder, CO 80303

[6]Department of Molecular, Cellular, and Developmental Biology, University of Colorado, Boulder, Colorado 80309, USA.

[7]Department of Ecology and Evolutionary Biology, University of Colorado, Boulder, CO 80309

Corresponding authors:

paulcarini@email.arizona.edu or noah.fierer@colorado.edu

Keywords: Microbial seasonality, soil microbial ecology, microbial interactions

Abstract:

Few studies have comprehensively investigated the temporal variability in soil microbial communities despite widespread recognition that the belowground environment is dynamic. In part, this stems from the challenges associated with the high degree of spatial heterogeneity in soil microbial communities[1] and because the presence of relic DNA[2] may mask temporal dynamics. Here we disentangle the relationships among spatial, temporal, and relic DNA effects on microbial communities in soils collected from contrasting hillslopes in Colorado, USA. These sites were chosen because they have distinct soil microbial communities and experience strong seasonal changes in precipitation and temperature regimes. We intensively sampled plots on each hillslope over one year to discriminate between temporal variability, the intra-plot spatial heterogeneity, and relic DNA effects on the soil prokaryotic and fungal communities. We show that the intra-plot spatial variability in microbial community composition was strong and independent of relic DNA effects and these spatial patterns persisted throughout the study. When controlling for intra-plot spatial variability, we identified significant temporal variability in both plots, particularly after relic DNA was removed, suggesting that relic DNA hinders the detection of important temporal dynamics in soil microbial

communities. We also identified microbial taxa that exhibited shared temporal responses and we show that these responses were often predictable from temporal changes in soil conditions. These findings highlight approaches that can be used to better characterize temporal shifts in soil microbial communities, information that is critical for predicting the environmental preferences of individual soil microbial taxa and identifying linkages between soil microbial community composition and belowground dynamics.

Introduction:

Information on the temporal dynamics of microbial communities over different time scales can be used to better understand the factors influencing the structure of microbial communities and their contributions to ecosystem processes. We know that the microbial communities found in the human gut[3], leaf litter[4], marine[5], and freshwater[6] habitats can exhibit a high degree of temporal variation. Although the magnitude and timing of this temporal variation in community composition can vary depending on the environment and taxon in question, such temporal variability is often predictable from environmental factors[7]. For example, ocean microbial communities display predictable periodic oscillations over time (seasonality) that has been linked to regular changes in biotic and abiotic factors, including phytoplankton dynamics and physicochemical factors (reviewed in refs [5,8]). These changes in environmental conditions influence the nature of biotic interactions within these ecosystems and can have important ramifications for understanding the functional attributes of microbial communities and the ecosystem services they provide[9-11].

Understanding how temporal changes in environmental conditions influence soil microbial communities is necessary to accurately model how microbial communities contribute to soil processes and for using microbes as bio-indicators of changes in belowground conditions such as carbon and nutrient availability – parameters that are often difficult to measure directly. However, results from previous studies of temporal variability in soil microbial communities are idiosyncratic. While some studies show soil microbial communities exhibit measurable temporal variation in response to experimental warming[12,13] and seasonal patterns in temperature and moisture[14-18], other studies show no or minimal variation over time, despite marked changes in environmental conditions[7,19,20]. One possible explanation for the discrepancies across studies is that the spatial heterogeneity in soil microbial communities – even across short distances – can be sufficiently large to obscure temporal patterns. This hypothesis is supported by numerous studies demonstrating that the spatial variability in soil microbial communities (even across locations only a few meters apart) can be large (for example, ref. [1]). Another explanation is that relic DNA – legacy DNA from dead microbes that can persist in soil – may dampen the observed temporal variability by effectively hiding the true temporal dynamics of soil microbial communities. Relic DNA is abundant in soil[2,21], and models suggest that during microbial community turnover relic DNA can mask changes in community structure[21].

We conducted a yearlong study aimed at disentangling the spatial and relic DNA effects on temporal dynamics in belowground microbial communities. Our study sites were soils on opposing hillslope aspects of a montane ecosystem within the Colorado Front Range of the Rocky Mountains. We intensively sampled two 9 m × 9 m plots,

divided into 3 m × 3 m sub-plots, located in the Gordon Gulch subcatchment within the Boulder Creek Critical Zone Observatory (BcCZO) every 40-55 days from November 2015 to November 2016 (Fig. 1; nine time points total). We chose these locations because the soil microbial communities on the two hillslopes are compositionally distinct[2], relic DNA is abundant (40-60% of the total soil DNA pool, ref. [2]), and the two sites undergo strong seasonal changes in moisture and temperature[22]. Moreover, the temperature and moisture regimes are distinct across the two slopes[22], providing us with naturally contrasting systems in which to investigate temporal dynamics in belowground microbial communities. We characterized the microbial communities at each site using 16S rRNA gene and internal transcribed spacer 1 (ITS) marker sequencing to profile the prokaryotic and fungal communities, respectively. Here, we unravel the relationships between spatial and temporal variability in microbial community composition, and show the effects of relic DNA on these apparent sources of variability. Further, we use this information on temporal dynamics to identify groups of microbes that share temporal patterns and similar responses to changes in environmental conditions, information that provides novel insight into the ecologies of understudied soil microbial taxa.

Results & Discussion:

Spatial variation in soil microbial communities is unaffected by relic DNA and stronger than temporal variation. Consistent with previous studies conducted at these sites[2], and other studies describing the spatial variability of soil microbial communities[1], the prokaryotic and fungal communities on the south-facing hillslope (SFS) were distinct from those on the north-facing hillslope (NFS), regardless of the time point sampled or whether relic DNA was removed (Supplementary Fig. 1). Most notably, the SFS had higher relative abundances of the archaeal phylum Crenarchaeota (all of which were classified as probable ammonia-oxidizing '*Candidatus* Nitrososphaera'), and the bacterial phyla Nitrospirae and Verrucomicrobia (Supplementary Fig. 2). Beyond these expected slope-scale differences, we observed significant intra-plot spatial heterogeneity in microbial community composition that persisted throughout the course of the experiment, and this intra-plot heterogeneity was evident irrespective of whether relic DNA was removed. Before removing relic DNA, there was significant spatial variability across the sub-plots in both prokaryotic and fungal communities on the NFS (Fig. 2 a,e; PERMANOVA R^2=0.192 and R^2=0.328; P≤0.001, respectively). Significant spatial differences were still apparent on the NFS for both prokaryotes and fungi after relic DNA was removed (Fig. 2 c,g; PERMANOVA R^2=0.180 and R^2=0.287; P≤0.001, respectively). We also found significant spatial variability on the SFS in samples that were not treated to remove relic DNA, but this spatial effect was much more pronounced than the NFS, with a clear partitioning between sub-plots 5, 6, 8 and 9 (see 'Plot Design' in Fig. 1a for numbering) from the remainder of the sub-plots (Fig. 2 b,f; PERMANOVA R^2=0.511, P≤0.001 for prokaryotes and R^2=0.331, P≤0.001 for fungi). Similar to the NFS, these strong spatial patterns remained after relic DNA was removed (Fig. 2 d,h; PERMANOVA R^2=0.498 for prokaryotes and R^2=0.290 for fungi; P≤0.001). These data show that the spatial variability in soil microbial community composition on the meter scale persists over time and that the presence of relic DNA does not affect our ability to detect this persistent spatial variation.

Removing relic DNA enhanced our ability to detect temporal changes in soil microbial communities. We investigated the temporal variability in belowground microbial communities, and the effect of relic DNA on this temporal variability, on a sub-plot basis to control for the aforementioned high degree of intra-plot spatial variability and discriminate between temporal and spatial sources of variation in microbial community structure. When limiting PERMANOVA permutations to within sub-plots over time, we found significant temporal variability for both prokaryotes and fungi in both untreated control soils (PERMANOVA R^2 =0.187 P≤0.001 for prokaryotes and R^2 =0.147 P≤0.001 for fungi on the NFS; and R^2 =0.123 P≤0.001 for prokaryotes and R^2 =0.123 P≤0.001 for fungi on the SFS) and soils that were treated to remove relic DNA (PERMANOVA R^2 =0.177 P≤0.001 for prokaryotes and R^2 =0.141 P≤0.001 for fungi on the NFS; and R^2 =0.108 P≤0.001 for prokaryotes and R^2 =0.157 P≤0.001 for fungi on the SFS). However, on average, the fungal communities on both slopes, and prokaryotic communities on the NFS were significantly more dissimilar over time after relic DNA was removed, compared to untreated control soils that contained relic DNA (Fig. 3; Kruskal-Wallis test P≤0.05). These results indicate that, while temporal signals in soil microbial communities can be identified in the presence of relic DNA, the removal of 'legacy' DNA from dead microbes that can persist in soil significantly enhances the ability to detect important temporal variation in the composition of soil microbial communities.

Temporal variability in distinct assemblages of prokaryotes and fungi are predictable from soil variables. Characterizing shifts in the relative abundances of individual microbial taxa in temporally dynamic soil systems can give important insight into the ecologies of individual taxa and, more generally, the environmental factors that influence belowground communities. Thus, we next sought to identify specific groups of taxa that exhibited correlated changes in relative abundances over time in soils after relic DNA was removed. To do this, we used local similarity analysis (LSA)[23] to identify strong (local similarity score ≥0.7) and significant (q-value ≤0.001) positive pairwise microbe-microbe temporal correlations. We constructed and analyzed networks from these correlations and extracted distinct groups (modules) of microbes from NFS and SFS networks using modularity analysis[24] (Fig. 4). On the NFS, the mean normalized relative abundances of 292 microbial taxa (184 bacteria and 108 fungi) were significantly correlated with at least one other taxon over time (Fig. 4a). These correlated taxa clustered into seven modules – the mean normalized relative abundances of four of these modules changed significantly with time and displayed distinct temporal trajectories (Fig. 4b). On the SFS, 291 taxa (1 archaeon, 191 bacteria and 99 fungi) were included in the network, and clustered into six modules (Fig. 4c). The relative abundances of three of these six SFS modules changed significantly with time (Fig. 4d).

A large proportion of the temporal variation in the mean normalized relative abundances of the modules that were found to change significantly over time could be explained by temporal variation in measured soil or environmental characteristics. At each time point, we measured a suite of soil and environmental parameters, including: snow depth, soil temperature and moisture, extractable inorganic nitrogen (NO_3^- +

185 NH_4^+), salinity (electrical conductivity), extractable phosphorus (P), pH, and the
186 chromophoric properties of water-soluble organic matter (WSOM; a metric of organic
187 matter lability[25]). These measured soil characteristics explained 12 to 76% of the
188 variance in the mean normalized relative abundance of a given module (Supplementary
189 Fig. 3). We identified two sets of modules that differed in the specific factors that
190 predicted temporal variation. The first set of modules, containing modules 0, 3, 7 and
191 12, were best predicted by climactic variables, most notably soil temperature and
192 moisture and snow depth (Supplementary Fig. 3). These results are in line with previous
193 studies demonstrating how changes in soil temperature[12,16-18], moisture[26] and snow
194 pack[14] can influence belowground microbial communities. In contrast, modules 1, 2 and
195 11 were best explained by changes in inorganic nutrient concentrations (nitrogen and
196 phosphorus; Supplementary Fig. 3). While nitrogen and phosphorus inputs can have
197 predictable[27] and lasting[4] effects on microbial community structure, we have a more
198 limited understanding of how short-term seasonal variation in the availability of these
199 nutrients can influence microbial community dynamics, despite evidence that
200 belowground microbial communities are important mediators of soil nutrient
201 dynamics[28,29]. Our results show that a subset of soil microbes organize into modules
202 that are responsive to these subtle changes in nitrogen and phosphorus availability.
203 Variability in WSOM constituents did not contribute significantly to temporal variability in
204 environmental conditions (Supplementary Fig. 4) and thus, we excluded these
205 measures from the models describing the temporal variability of the modules. Given that
206 previous work at these sites showed a high degree of spatial variation in WSOM
207 distributions[25,30], we suspect that the pronounced spatial variability in WSOM
208 distributions may have obscured our ability to detect significant effects of WSOM
209 characteristics on the temporal dynamics of the soil microbial communities.
210 The construction of modules based on shared temporal patterns allowed us to
211 identify biotic or abiotic factors that are correlated with shifts in the relative abundances
212 of individual taxa. For example, similar to studies showing that ammonia-oxidizing
213 archaea are particularly sensitive to changes in temperature[31] and pH[32,33], we found that
214 both temperature and pH were good predictors of the temporal distribution of module
215 12, which contained ammonia-oxidizing thaumarchaea (Fig. 4d and Supplementary Fig.
216 3). Because nitrification is often a coupled process – the oxidation of ammonium to
217 nitrite by ammonia oxidizers, and the subsequent oxidation of nitrite to nitrate by nitrite
218 oxidizers – we were surprised that probable nitrite-oxidizing Nitrospirae were not
219 temporally correlated with these thaumarchaea, but were instead a part of a distinct
220 module (module 8; Fig. 4d) that did not change significantly over time. As observed in
221 some marine systems[34,35], we suspect that nitrification in SFS soils may be periodically
222 uncoupled, though more work is necessary to test this hypothesis.
223 Our study also provides insight into the short-term temporal variation of
224 ectomycorrhizal communities, the environmental factors that influence these patterns
225 and other fungal and prokaryotic taxa that co-vary with ectomycorrhizal fungi.
226 Ectomycorrhizal fungi were found on both slopes and partitioned into several modules
227 that were significantly variable over time (modules 0, 1, 2, 3, 7, 11, and 12 in Fig. 4;
228 Supplementary Table 1). Interestingly, some of these modules were best predicted by
229 climactic variables (Supplementary Fig. 3; for example, those ectomycorrhizal fungi
230 found in modules 3 and 7). Modules 3 and 7 had peak abundances in the summer

231 months (Fig. 4), suggesting that the abundances of these ectomycorrhizal taxa were
232 elevated during months when plant productivity peaks. However, other ectomycorrhizal
233 fungi were found in modules best predicted by nutrient availability. These findings
234 indicate a degree of temporal niche partitioning in ectomycorrhizal fungal communities
235 on both slopes in response to distinct environmental conditions (Supplementary Fig. 3)
236
237 **Conclusions:**
238 This study provides new evidence that the temporal dynamics of groups of
239 prokaryotes and fungi are predictable in terrestrial ecosystems, and that a more detailed
240 characterization of the temporal variability in soil microbial communities is critical to
241 understanding the dynamic nature of the soil microbiome. The extensive spatial and
242 temporal sampling design of our study allowed us to disentangle the relationships
243 among spatial heterogeneity in microbial communities, temporal dynamics of these
244 communities, and the effect of relic DNA on these temporal patterns. Unsurprisingly,
245 spatial variation in community structure at both the hillslope scale, and the meter scale
246 (intra-plot) was the dominant source of variability in this study and relic DNA had no
247 significant effect on these patterns (Supplementary Fig. 1 and Fig. 2).
248 When controlling for this spatial variability, we were able to detect significant
249 temporal shifts in microbial community composition, regardless of whether relic DNA
250 was removed or not. We emphasize that the magnitude of the temporal variation in soil
251 microbial communities was consistently lower than the spatial variation, even between
252 sub-plots located only a few meters apart. This spatial variability in surface soil microbial
253 communities was relatively stable over time, suggesting that efforts to describe spatial
254 variation in overall community composition do not necessarily need to include samples
255 collected across multiple time points.
256 We also provide new evidence that the removal of relic DNA enhances our ability to
257 detect temporal patterns in the belowground communities. These findings support our
258 previous hypothesis[2], and predictions based on modeling[21], that relic DNA can conceal
259 temporal patterns in soil microbial communities. The presence of relic DNA, even in high
260 amounts, does not automatically lead to relic DNA biases in other ecosystems[21].
261 However, our data do suggest that relic DNA has important effects on studies of
262 temporal variation in soil microbial communities (and possibly in other ecosystems), and
263 that the consequences of failing to remove relic DNA would not be apparent from single
264 time point samples.
265 The belowground environment is one of the most complex and dynamic microbial
266 habitats on Earth. By controlling for spatial and relic DNA effects on temporal variability
267 in these soil microbial communities, we identified groups of microbes that have similar
268 temporal dynamics and the factors that predicted their temporal distributions. A deeper
269 understanding of relationships between soil microbiota can help resolve both the roles
270 of individual taxa and potential 'ecological clusters' with emergent function. For
271 example, taxa that covary may exhibit similar niche preferences and compete for growth
272 substrates. In contrast, taxa belonging to a given module may broadly cue in on similar
273 environmental signals but occupy distinct substrate niches[36]. Alternatively, microbes that
274 are correlated over time may interact through cross-feeding of metabolic substrates or
275 co-utilization of leaky functions[37] - either directly or in a time-lagged manner.
276 Understanding the basis for shared temporal dynamics is important as microbial

interactions are crucial in shaping microbial communities[38] but difficult to measure directly[39]. Future investigations that combine cell culture, synthetic microbial communities and genomics may help resolve the specific drivers of these co-occurrence patterns[36,40].

Methods:

Site description, plot design and sampling procedure: The two plots were set up on opposing slopes alongside an instrumented transect near the rain-snow transition at ~2,530 meters elevation (approximately 40.01°N, 105.47°W), chosen on the expectation that there would be a high level of temporal variability in soil microbial communities as a result of intra-annual changes in soil moisture and temperature[22]. The north-facing slope (NFS) and south-facing slope (SFS) have distinct soil and vegetation characteristics and experience different water delivery patterns, particularly during snowmelt[22] (Fig. 1). The NFS and SFS soils are Ustic dystrocryept (Catamount series) and Lithic haplstoll, respectively[41]. Soil moisture and temperature were variable over the course of the study and followed expected seasonal trends (Fig. 1). In general, the NFS had a higher soil moisture and a lower temperature than the SFS (Fig. 1). The NFS is vegetated with moderately dense *Pinus contorta* (Lodgepole pines) and develops a snowpack during the winter that melts in spring. In contrast, the SFS is much more sparsely vegetated with *Pinus ponderosa* (Ponderosa pines), intervening grasses and *Arctostaphylos uva-ursi* (kinnikinnick) shrubs and experiences pulses of snowmelt throughout the winter and spring. We sampled ~10-15 random soil cores (0-5 cm, mineral soils only; 1" core diameter) within each sub-plot at each of the nine time points. The soil cores from each sub-plot were pooled, sieved to 2 mm and homogenized at each time point and partitioned for microbial community and nutrient analyses. Sample dates are reported in Supplementary Table 2. Sampling for the July 2016 sample was delayed by ~7 days because a nearby wildfire prevented site access.

Continuous environmental measurements: Several automated measurements were collected every 10 minutes at a meteorological station located near the sample sites (see 'Data availability' for data source information). Each slope was instrumented with a soil temperature sensor (Campbell Scientific T-107 temperature probe), and a soil water content reflectometer (Campbell Scientific CS616) located 5 cm below ground. The daily averages from these sensors on each slope are illustrated in Fig. 1b,c. When modelling the relative mean importance of temperature and volumetric water content to module temporal distributions, we used the average of daily mean values from these sensors between sample dates, except for the first time point, which is the mean from the preceding 34 days. Snow depth was measured using digital ultrasonic snow depth sensors (Judd Communications Inc.) fitted with CR1000 dataloggers (Campbell Scientific). Snow depth is reported as mean daily snow depth between sampling points from three sensors on each slope (NFS at snow pole 3, sensors 1-3 and SFS snow pole 10, sensors 9, 11 and 15).

Discrete environmental measurements: Inorganic N pools were measured for each sub-plot at each time point except for the January 2016 sample on the NFS, sub-plots 1 and 2 and SFS sub-plot 3, where insufficient soil was collected. Sieved soils for

inorganic N analyses were stored at 4°C for <72 h. Inorganic N pools were extracted from 10 g field-moist soil in 100 mL 2M potassium chloride with periodic shaking for 18 h and filtered through cellulose Whatman 1 filters. Ammonium (NH_4^+) was measured from these extracts on a BioTek Synergy 2 with a detection limit of 0.009 mg N L^{-1} and nitrate (NO_3^-) was measured on an OI Analytical FS-IV with a detection limit of 0.5603 µg N L^{-1}. Dissolved inorganic nitrogen (DIN) was calculated as the sum of NH_4^+ and NO_3^-.

Water-soluble organic matter (WSOM) was analyzed for each sub-plot at each time point except for the following plots, where insufficient sample was collected: NFS February 2016 (all sub-plots), July 2016 sub-plot 1, August 2016 sub-plots 1-7, November 2016 sub-plots 1, 2 and 5; and SFS February 2016 sub-plots 1, 8 and 9 and April 2016 sub-plot 5. Sieved soils were stored at -20°C until WSOM extraction. WSOM was extracted by leaching 10 g of soil with 50 ml 0.5 M K_2SO_4 following the methods described in[25]. The spectroscopically-active portion of the WSOM was characterized with UV-Vis and fluorescence spectroscopy. Samples were diluted to minimize the inner filter effect[42] and the UV-Vis absorbance was measured from 200-800 nm in 1 nm increments using an Agilent 8453 Spectrophotometer with a 1 cm path length. Dissolved organic carbon (DOC) and total nitrogen were measured on a Shimadzu TOC-V. $SUVA_{254}$, a proxy for the aromaticity of the WSOM, was calculated as the absorbance at 254 nm normalized by the DOC concentration[43]. Fluorescence scans were collected on a Horiba Jobin Yvon Fluoromax-4 with a 1 cm quartz cuvette and normalized to Raman units[44]. The fluorescence index (FI) [45] and humification index (HIX)[46] were calculated from the fluorescence scans using Parallel Factor Analysis (PARAFAC) to further resolve discrete components representing different classes of fluorophores[25].

Other standard soil characteristics were measured at each time point by pooling equal masses of soil from each sub-plot plot on each slope. These measurements included: pH, electrical conductivity (mmhos cm^{-1}) and P (ppm). Standard soil chemical analyses were performed at the Colorado State University Soil Water and Plant Testing Laboratory using their standard protocols.

Relic DNA removal and DNA extraction: Relic DNA was removed as described previously[2]. Briefly, 0.03 g of each soil from each sub-plot pool was sub-sampled, resuspended in 3.0 mL phosphate buffered saline (PBS) (1% weight/vol slurry) and either treated with 40 µM propidium monoazide (PMA) in the dark, or left untreated as a control. Both treated and untreated samples were vortexed in the dark for 4 minutes and exposed to a 650-watt light for 4 × 30 s light:30 s dark cycles to activate PMA in treated samples. Light-exposed samples were frozen at -20°C until DNA extraction. DNA was extracted from 800 µL of PMA treated and untreated soil slurries using a PowerSoil-htp 96 well soil DNA Isolation kit (MoBio) following the manufacturer's instructions, except 770 µL was used in the C2 step. All samples and 27 'no soil' negative controls were randomized into these 96 well DNA extraction plates and extracted simultaneously.

Amplicon sequencing and analytical methods: For sequence-based analyses of 16S rRNA and ITS marker regions, we used the approaches described previously[2]. Briefly, we amplified each sample in duplicate in 25 µl PCR reactions containing: 12.5 µl of Promega GoTaq Hot Start Colorless Master Mix; 0.5 µl of each barcoded primer (bacterial 16S: 515F 5'-GTGCCAGCMGCCGCGGTAA-3' & 806R 5'-

GGACTACHVGGGTWTCTAAT-3'; fungal ITS: 5′-CTTGGTCATTTAGAGGAAGTAA-3′ & ITS2 5′-GCTGCGTTCTTCATCGATGC-3′); 10.5 µl water; 1 µl of template DNA. Program: 94°C for 5 min, followed by 35 cycles of (94°C 45 s; 50°C 60 s; 72°C 90 s) and a final extension 72°C 10 min. Duplicate PCR reactions for each sample were pooled, cleaned and normalized using the ThermoFisher Scientific SequalPrep Normalization Plate kit. Cleaned and normalized amplicons were pooled, spiked with 15% phiX and sequenced on an Illumina MiSeq using v2 500-cycle paired end kits. The samples were sequenced in four batches total – two for prokaryotes and two for fungi. The first two sequencing runs (one each for prokaryotes and fungi) contained all treatments and control samples up to and including the May 2016 samples. The last two sequencing runs (one each for prokaryotes and fungi) two contained samples collected on July 2016 and thereafter, plus control samples. We analyzed the 'no soil' controls to determine whether there were potential sequencing batch effects across the runs for prokaryotes or for fungi that could be detected in the community composition of these controls. We found no significant difference in the 'no soil' controls for prokaryotes (rarified to 89 reads to include all controls; PERMANOVA R^2=0.028; P=0.677) or fungi (not rarified to include all controls; PERMANOVA R^2=0.028 P=0.613) that would be indicative of batch effects. Reads were processed as described in (ref. [27]). Briefly, raw amplicon sequences were demultiplexed according to the raw barcodes and processed with the UPARSE pipeline[47]. A database of ≥97% similar sequence clusters was constructed in USEARCH (Version 8)[48] by merging paired end reads, using a "maxee" value of 0.5 when quality filtering sequences, dereplicating identical sequences, removing singleton sequences, clustering sequences after singleton removal, and filtering out cluster representative sequences that were not ≥75% similar to any sequence in Greengenes (for prokaryotes; Version 13_8)[49] or UNITE (for fungi)[50] databases. Demultiplexed sequences were mapped against the *de novo* constructed databases to generate counts of sequences matching clusters (i.e. taxa) for each sample. Taxonomy was assigned to each taxon using the RDP classifier with a threshold of 0.5[51] and trained on the Greengenes or UNITE databases. To normalize the sequencing depth across samples, samples were rarefied to 10,159 and 5,000 sequences per sample for the 16S rRNA and ITS analyses, respectively. Functional predictions for fungal taxa were obtained using FUNGuild[52].

Statistical analyses: Calculations of community dissimilarity and all other analyses were conducted on a reduced dataset because of the spatial and temporal heterogeneity. That is, we wanted to understand the temporal variation of microbes that are consistently present across the sub-plots and over time. When comparing slope differences, we included only taxa that were present on at least one slope *i*) with a mean read abundance of greater than 81 or 40 reads after rarefaction, for prokaryotes and fungi, respectively across all samples (an average of one (prokaryotes) or 0.5 (fungi) reads per sub-plot, per time point); and were *ii*) present in more than 27 samples (1/3 of all samples). Second, we investigated only those taxa that were, on average, ≥ 0.1% of the community across all samples. When investigating within-plot differences, we focused on only the taxa within that plot that met the above parameters. We emphasize that these filtering steps were deliberately stringent to enable robust temporal analyses of taxa that are consistently present both spatially and temporally. Bray-Curtis distances were calculated on this subset using the mctoolsr R package.

Bray–Curtis dissimilarities were calculated on square root transformed taxon relative abundances.

Temporal analyses and network construction: We identified significant temporal correlations in the relative abundances of individual taxa derived from soils that were treated to remove relic DNA using extended Local Similarity Analysis (eLSA)[23] with the following parameters: `lsa_compute -s 9 -r 9 -p perm`. We defined significant temporal associations as those with a local similarity (LS) score ≥0.7 (i.e.-strong to very strong correlations) and a *q* value ≤ 0.001. Pairs of significantly correlated taxa were analyzed in Gephi (version 0.8.2). Network modularity was calculated by implementing the 'modularity' function[24] built in within Gephi, with a resolution setting of 1.0 for both slopes. Node IDs (individual taxa) belonging to the same module were extracted to delineate temporal patterns. Normalized relative abundances for each node ID were calculated using the tRank command in the multic R package.

Random forest analysis: For each slope, we used Random Forest[53] modeling to first identify those measured environmental and soil variables that were significant (P ≤ 0.05) predictors of time, using time as a response variable (Supplementary Fig. 4). These significant environmental factors are expected to predict changes in module abundance over time (Supplementary Fig. 3). We then conducted a second round of Random Forests analysis with the significant environmental predictors to identify the most important environmental factors or soil characteristics that predicted the mean normalized relative abundances of each module (see ref. [54] for a similar approach). The importance (increase in mean square error %) and significance of each predictor was computed for each tree and averaged over the forest (9999 trees) using the rfPermute R package. Significant predictors were defined as those with a *P* value ≤ 0.05. Samples for which environmental and soil characteristics were missing because of insufficient sample were excluded from random forest and spearman correlation analysis.

Data Availability: Raw DNA sequence data, the corresponding mapfile and all soil and environmental characteristics are available on figshare.com: 10.6084/m9.figshare.6710087. Snow depth data are available through the Boulder Creek Critical Zone Observatory website: http://criticalzone.org/boulder/data/dataset/2423/. Temperature data for the NFS and SFS are available through the Boulder Creek Critical Zone Observatory website http://criticalzone.org/boulder/data/dataset/2426/.

References:

1. O'Brien, S. L. *et al.* Spatial scale drives patterns in soil bacterial diversity. *Environmental Microbiology* **18,** 2039–2051 (2016).
2. Carini, P. *et al.* Relic DNA is abundant in soil and obscures estimates of soil microbial diversity. *Nature Microbiology* **2,** 1–6 (2016).
3. Flores, G. E. *et al.* Temporal variability is a personalized feature of the human microbiome. *Genome Biology* **15,** 531 (2014).
4. Matulich, K. L. *et al.* Temporal variation overshadows the response of leaf litter microbial communities to simulated global change. *The ISME Journal* **9,** 2477–2489 (2015).

5. Giovannoni, S. J. & Vergin, K. L. Seasonality in ocean microbial communities. *Science* **335,** 671–676 (2012).
6. Newton, R. J., Kent, A. D., Triplett, E. W. & McMahon, K. D. Microbial community dynamics in a humic lake: differential persistence of common freshwater phylotypes. *Environmental Microbiology* **8,** 956–970 (2006).
7. Shade, A., Caporaso, J. G., Handelsman, J., Knight, R. & Fierer, N. A meta-analysis of changes in bacterial and archaeal communities with time. **7,** 1493–1506 (2013).
8. Fuhrman, J. A., Cram, J. A. & Needham, D. M. Marine microbial community dynamics and their ecological interpretation. *Nature Reviews Microbiology* **13,** 133-146 (2015).
9. Penton, C. R. *et al.* Denitrifying and diazotrophic community responses to artificial warming in permafrost and tallgrass prairie soils. *Front. Microbiol.* **6,** 439–13 (2015).
10. Needham, D. M. & Fuhrman, J. A. Pronounced daily succession of phytoplankton, archaea and bacteria following a spring bloom. *Nature Microbiology* **1,** 1–7 (2016).
11. Li, X. *et al.* Changes in the structure and function of microbial communities in drinking water treatment bioreactors upon addition of phosphorus. *Applied and Environmental Microbiology* **76,** 7473–7481 (2010).
12. DeAngelis, K. M. Long-term forest soil warming alters microbial communities in temperate forest soils. **6,** 104 (2015).
13. Zhang, N., Xia, J., Yu, X., Ma, K. & Wan, S. Soil microbial community changes and their linkages with ecosystem carbon exchange under asymmetrically diurnal warming. *Soil Biology and Biochemistry* **43,** 2053–2059 (2011).
14. Schadt, C. W., Martin, A. P., Lipson, D. A. & Science, S. S. Seasonal dynamics of previously unknown fungal lineages in tundra soils. *Science* **301,** 1359–1361 (2003).
15. Kennedy, N., Brodie, E., Connolly, J. & Clipson, N. Seasonal influences on fungal community structure in unimproved and improved upland grassland soils. *Canadian Journal of Microbiology* **52,** 689–694 (2006).
16. Lipson, D. A., Schadt, C. W. & Schmidt, S. K. Changes in soil microbial community structure and function in an alpine dry meadow following spring snow melt. *Microb. Ecol.* **43,** 307–314 (2002).
17. Lipson, D. A. Relationships between temperature responses and bacterial community structure along seasonal and altitudinal gradients. *FEMS Microbiology Ecology* **59,** 418–427 (2006).
18. Lipson, D. A. & Schmidt, S. K. Seasonal changes in an alpine soil bacterial community in the Colorado Rocky Mountains. *Applied and Environmental Microbiology* **70,** 2867–2879 (2004).
19. Docherty, K. M. *et al.* Key edaphic properties largely explain temporal and geographic variation in soil microbial communities across four biomes. *PLoS ONE* **10,** e0135352–23 (2015).

20. Bond-Lamberty, B. *et al.* Soil respiration and bacterial structure and function after 17 years of a reciprocal soil transplant experiment. *PLoS ONE* **11,** e0150599–16 (2016).
21. Lennon, J. T., Muscarella, M. E., Placella, S. A. & Lehmkuhl, B. K. How, when, and where relic DNA affects microbial diversity. *mBio* **9,** e00637–18–14 (2018).
22. Hinckley, E.-L. S. *et al.* Aspect control of water movement on hillslopes near the rain-snow transition of the Colorado Front Range. *Hydrol. Process.* **28,** 74–85 (2012).
23. Xia, L. C. *et al.* Extended local similarity analysis (eLSA) of microbial community and other time series data with replicates. *BMC Syst Biol* **5** S15–S15 (2011).
24. Blondel, V. D., Guillaume, J.-L., Lambiotte, R. & Lefebvre, E. Fast unfolding of communities in large networks. *Journal of Statistical Mechanics: Theory and Experiment* **10,** 10008 (2008).
25. Gabor, R. S. *et al.* Influence of leaching solution and catchment location on the fluorescence of water-soluble organic matter. *Environ. Sci. Technol.* **49,** 4425–4432 (2015).
26. Brockett, B. F. T., Prescott, C. E. & Grayston, S. J. Soil moisture is the major factor influencing microbial community structure and enzyme activities across seven biogeoclimatic zones in western Canada. *Soil Biology and Biochemistry* **44,** 9–20 (2012).
27. Leff, J. W. *et al.* Consistent responses of soil microbial communities to elevated nutrient inputs in grasslands across the globe. *Proc. Natl. Acad. Sci. U.S.A.* **112,** 10967–10972 (2015).
28. Spohn, M. *et al.* Temporal variations of phosphorus uptake by soil microbial biomass and young beech trees in two forest soils with contrasting phosphorus stocks. *Soil Biology and Biochemistry* **117,** 191–202 (2018).
29. Hinckley, E.-L. S., Barnes, R. T., Anderson, S. P., Williams, M. W. & Bernasconi, S. M. Nitrogen retention and transport differ by hillslope aspect at the rain-snow transition of the Colorado Front Range. *Journal of Geophysical Research: Biogeosciences* **119,** 1281–1296 (2014).
30. Gabor, R. S., Eilers, K., McKnight, D. M., Fierer, N. & Anderson, S. P. From the litter layer to the saprolite: Chemical changes in water-soluble soil organic matter and their correlation to microbial community composition. *Soil Biology and Biochemistry* **68,** 166–176 (2014).
31. Taylor, A. E., Giguere, A. T., Zoebelein, C. M., Myrold, D. D. & Bottomley, P. J. Modeling of soil nitrification responses to temperature reveals thermodynamic differences between ammonia-oxidizing activity of archaea and bacteria. *The ISME Journal* **11,** 896–908 (2016).
32. Stempfhuber, B. *et al.* pH as a Driver for ammonia-oxidizing archaea in forest soils. *Microb. Ecol.* **69,** 879–883 (2014).
33. Nicol, G. W., Leininger, S., Schleper, C. & Prosser, J. I. The influence of soil pH on the diversity, abundance and transcriptional activity of ammonia oxidizing archaea and bacteria. *Environmental Microbiology* **10,** 2966–2978 (2008).

34. Heiss, E. M. & Fulweiler, R. W. Coastal water column ammonium and nitrite oxidation are decoupled in summer. *Estuarine, Coastal and Shelf Science* **178,** 110–119 (2016).
35. Schaefer, S. C. & Hollibaugh, J. T. Temperature decouples ammonium and nitrite oxidation in coastal waters. *Environ. Sci. Technol.* **51,** 3157–3164 (2017).
36. Baran, R. *et al.* Exometabolite niche partitioning among sympatric soil bacteria. *Nature Communications* **6,** 8289 (2015).
37. Morris, J. J., Lenski, R. E. & Zinser, E. R. The Black Queen Hypothesis: Evolution of dependencies through adaptive gene loss. *mBio* **3,** e00036–12–e00036–12 (2012).
38. Bahram, M. *et al.* Structure and function of the global topsoil microbiome. *Nature* 1–24 (2018). doi:10.1038/s41586-018-0386-6
39. Faust, K. & Raes, J. Microbial interactions: from networks to models. *Nature Publishing Group* **10,** 538–550 (2012).
40. Zhalnina, K. *et al.* Dynamic root exudate chemistry and microbial substrate preferences drive patterns in rhizosphere microbial community assembly. *Nature Microbiology* **3,** 470–480 (2018).
41. Cole, J. C. & Braddock, W. A. *Geologic Map of the Estes Park 30□ X 60□ Quadrangle, North-central Colorado*. (2009).
42. Ohno, T. Fluorescence inner-filtering correction for determining the humification index of dissolved organic matter. *Environ. Sci. Technol.* **36,** 742–746 (2002).
43. Weishaar, J. L. *et al.* Evaluation of specific ultraviolet absorbance as an indicator of the chemical composition and reactivity of dissolved organic carbon. *Environ. Sci. Technol.* **37,** 4702–4708 (2003).
44. Lawaetz, A. J. & Stedmon, C. A. Fluorescence intensity calibration using the Raman scatter peak of water. *Appl Spectrosc* **63,** 936–940 (2009).
45. Cory, R. M. & McKnight, D. M. Fluorescence spectroscopy reveals ubiquitous presence of oxidized and reduced quinones in dissolved organic matter. *Environ. Sci. Technol.* **39,** 8142–8149 (2005).
46. Zsolnay, A., Baigar, E., Jimenez, M. & Steinweg, B. Differentiating with fluorescence spectroscopy the sources of dissolved organic matter in soils subjected to drying. *Chemosphere* **38,** 45–50 (1999).
47. Edgar, R. C. UPARSE: highly accurate OTU sequences from microbial amplicon reads. *Nat Meth* **10,** 996–998 (2013).
48. Edgar, R. C. Search and clustering orders of magnitude faster than BLAST. *Bioinformatics* **26,** 2460–2461 (2010).
49. McDonald, D. *et al.* An improved Greengenes taxonomy with explicit ranks for ecological and evolutionary analyses of bacteria and archaea. *The ISME Journal* **6,** 610–618 (2011).
50. Abarenkov, K. *et al.* The UNITE database for molecular identification of fungi--recent updates and future perspectives. *New Phytol.* **186,** 281–285 (2010).

595 51. Wang, Q., Garrity, G. M., Tiedje, J. M. & Cole, J. R. Naive Bayesian
596 classifier for rapid assignment of rRNA sequences into the new bacterial
597 taxonomy. *Applied and Environmental Microbiology* **73,** 5261–5267 (2007).
598 52. Nguyen, N. H. *et al.* FUNGuild: An open annotation tool for parsing fungal
599 community datasets by ecological guild. *Fungal Ecology* **20,** 241–248
600 (2016).
601 53. Breiman, L. Random Forests. *Machine Learning* **45,** 5–32 (2001).
602 54. Delgado-Baquerizo, M. *et al.* Differences in thallus chemistry are related to
603 species-specific effects of biocrust-forming lichens on soil nutrients and
604 microbial communities. *Funct Ecol* **29,** 1087–1098 (2015).
605
606
607 **Acknowledgements:** We thank Gordon Bowman, Youchao Chen, Matt Gebert,
608 Rebecca Gross, Evan Lih, Emily Morgan, Dillon Ragar, Nathan Rock and Joel Singley
609 for assistance setting up plots, sampling and nutrient analyses. We also thank David
610 Needham for assistance with LSA and Albert Barberán for critical feedback on the
611 manuscript. Funding to support this work was provided by grants from the National
612 Science Foundation EAR 1331828, EAR 1461281, and DEB 1556753 to N.F., and a
613 Visiting Postdoctoral Fellowship award to P.C. from the Cooperative Institute for
614 Research in Environmental Sciences at the University of Colorado.
615

Figures:

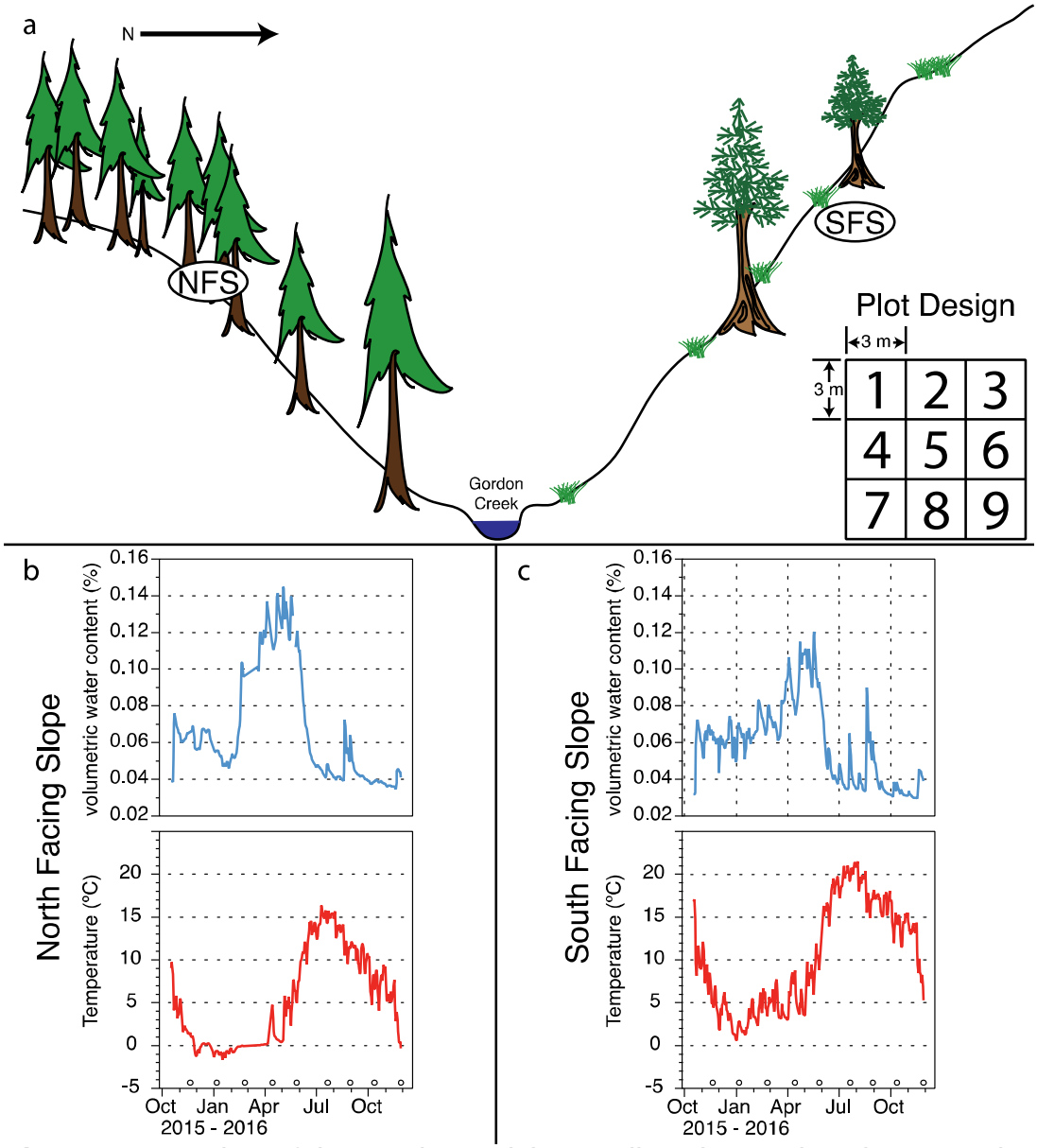

Figure 1: Overview of the Gordon Gulch sampling sites and environmental conditions across the sampling sites. (a) Conceptual diagram of sampling site location and plot design, reproduced with modification from[29]. The North facing slope (NFS) plot was centered at 40°0'44.759"N 105°28'9.123"W. The South facing slope (SFS) plot was centered at 40°0'48.551"N 105°28'8.355"W. Inset in (a) is an illustration of plot design. A single plot is comprised of nine 3 m × 3 m sub-plots. Numbers represent replicate sub-plots as described in the main text. Daily mean soil volumetric water content and soil temperature from *in situ* sensors at 5 cm depth for the NFS (b) and SFS (c) during the course of the experiment. Small circles on the temperature plots in (b) and (c) indicate sampling dates.

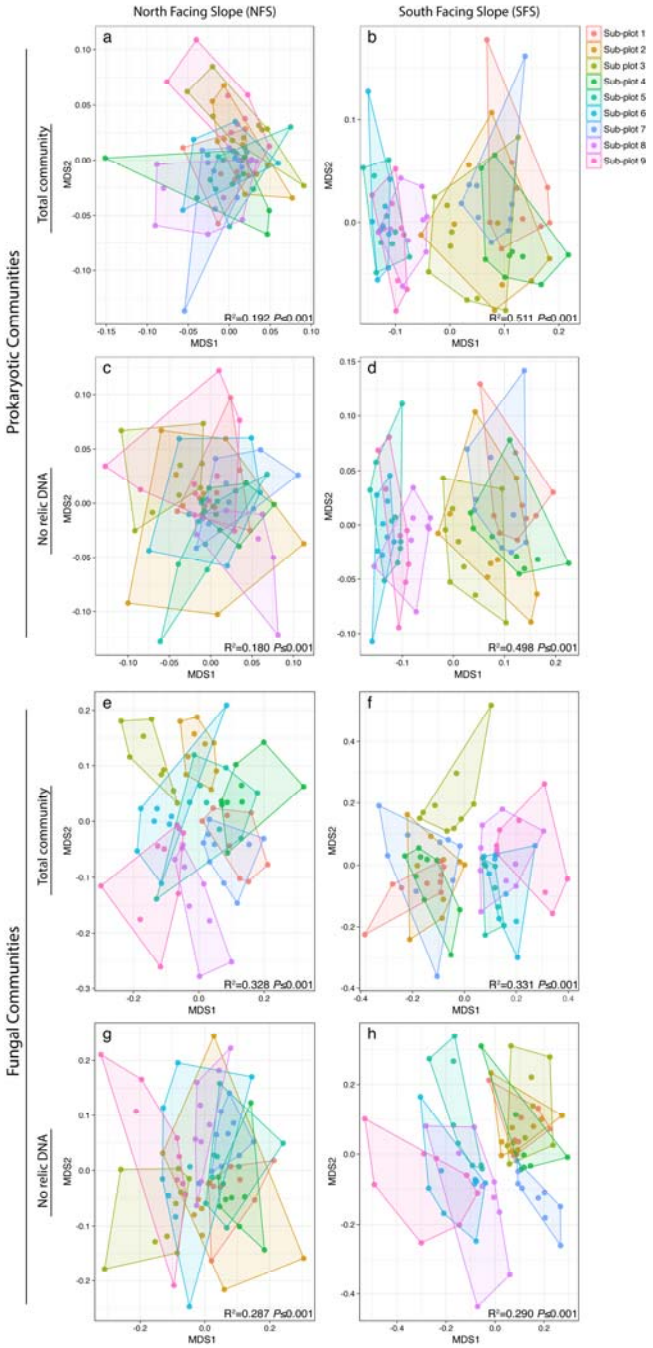

Figure 2: Intra-plot spatial variability in soil microbial communities persists over time on both slopes regardless of whether relic DNA is removed. NMDS plots showing the prokaryotic (a-d) or fungal (e-h) communities on the north facing slope (a,c,e,g) and south facing slope (b,d,f,h). Points are colored by sub-plot number (plot layout is illustrated in Figure 1 in the main text). Hulls connect the outermost points on each slope. PERMANOVA statistics are listed on each panel.

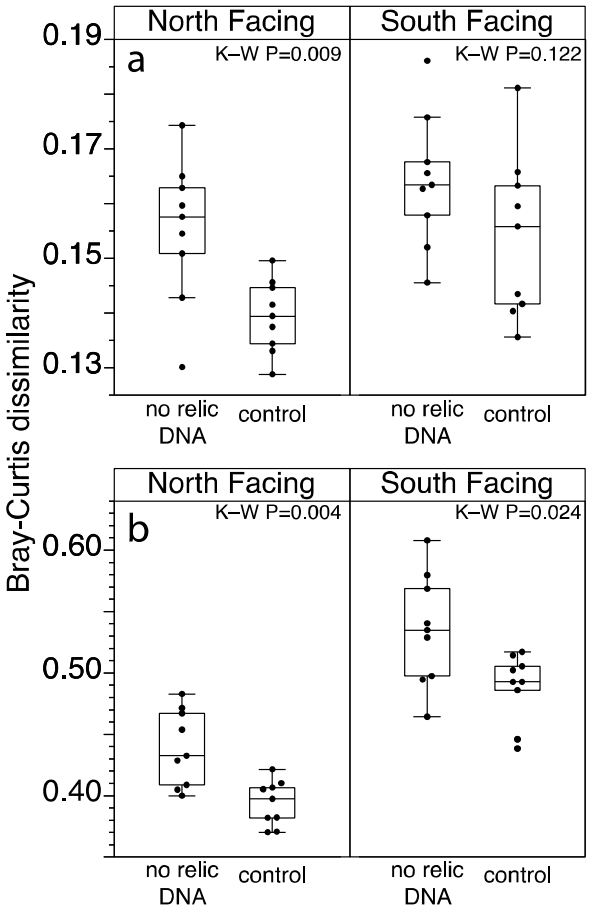

Figure 3: Soils without relic DNA were found to harbor microbial communities that are more dissimilar over time than in control soils containing relic DNA. (a) Prokaryotes (b) Fungi. Points are the mean community dissimilarity for a given sub-plot across all time points (n=9) for samples after relic DNA removal (no relic DNA) or untreated samples (control). Box plots illustrate interquartile range ± 1.5 × interquartile range. The horizontal line in each box plot is the median. Outliers (>1.5 × interquartile range) are shown as points outside of whiskers. Kruskal-Wallis test (K-W) P values are shown.

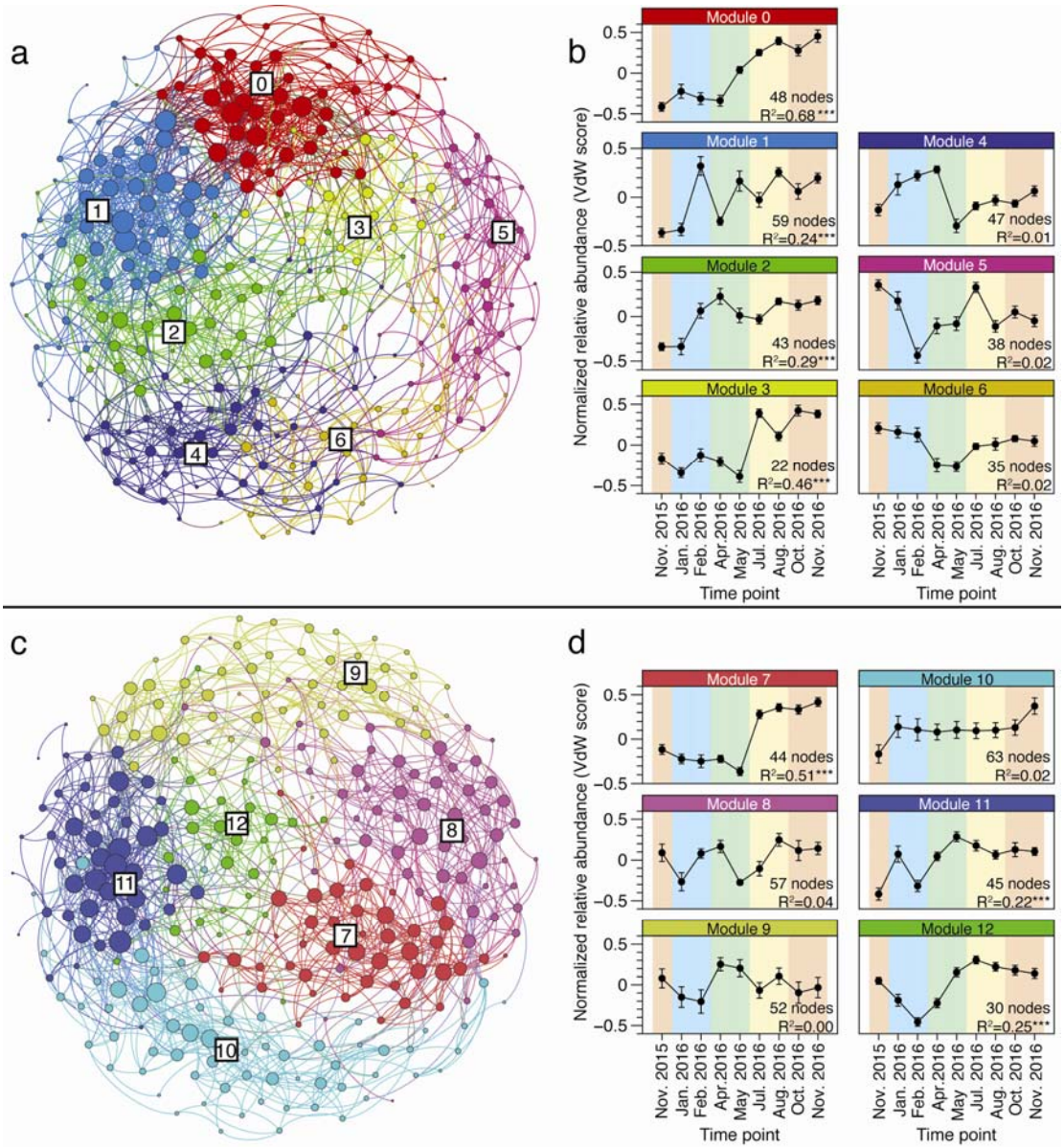

Figure 4: Cross-domain temporal dynamics in belowground microbial communities reveals temporal niche structure. Correlation networks based on significant microbe-microbe temporal correlations for the NFS (a) and SFS (c). Nodes in (a) & (c) are individual prokaryotic or fungal taxa. Lines between nodes represent significant (*q* value ≤ 0.001) and strong (local similarity score ≥ 0.7) positive temporal correlations. The sizes of nodes are proportional to the number of correlations to other nodes (the degree), whereby larger nodes have more connections. Colors represent distinct modules, as determined using the modularity algorithm described in ref. [24]. Boxed numbers in networks are arbitrary module numbers and match those in panels (b) and (d). Modularity analysis of each network revealed clusters of microbes that have similar temporal patterns. These temporal patterns were plotted for the NFS (b) and SFS (d). Points in (b) and (c) are the mean Van der Waerden (VdW) normalized relative abundance of all taxa in a given module. Error bars show ± SEM. The number of nodes included in each module and the PERMANOVA P value describing the relationship of

663 the normalized relative abundances in relation to time are shown. P values marked with
664 asterisks are significant at P≤0.001. Background is shaded by season: orange=autumn;
665 blue=winter; green=spring; yellow=summer. See Supplementary Table 1 for taxonomic
666 module membership.